

Three-dimensional electron density mapping of shape-controlled nanoparticle by focused hard X-ray diffraction microscopy

Metal nanostructures have been extensively studied for many decades because of their various applications. In general, the intrinsic properties of metal nanostructures can be tuned by controlling the shape as well as the structure of the nanostructures. Recently, extensive effort has been devoted to the synthesis of more complex structures, such as core-shell or hollow nanoparticles, because of their increased surface area, reduced densities, and localized surface plasmon resonance [1]. Determining the three-dimensional (3D) nano-mesoscopic structures is indispensable for a complete understanding of the structure-property relationship that guides the design and synthesis of nanomaterials with well-controlled sizes and shapes for specific applications.

X-ray diffraction microscopy is a lensless microscopy technique first demonstrated by Miao *et al.* in 1999 [2]. An object is illuminated with coherent X-ray beams and far-field diffraction data are collected by area detectors. Phase retrieval calculation is performed to reconstruct a 2D or 3D image. A number of applications of X-ray diffraction microscopy have emerged in biological and materials sciences. In principle, the spatial resolution of such diffraction microscopy is limited only by the wavelength of the incident beam. However, the spatial resolution achieved in experiments is effectively limited by the strong decay of the diffraction intensity with increasing scattering vector, and hence, high-flux-density coherent X-rays are crucial to improve the resolution. Recently, the spatial resolution has reached the sub-10-nm scale in two dimensions using focused high-density hard X-rays [3-5]. In addition, focusing

technologies for diffraction microscopy are also necessary to realize single-shot imaging using X-ray free electron lasers in the near future. In the present study [6], we first demonstrated 3D hard X-ray diffraction microscopy with a sub-10-nm scale resolution and revealed the 3D nano-mesoscopic structures of a shape-controlled Au/Ag nanobox.

Ag nanocubes with an edge length of ~150 nm were prepared by a modified polyol synthesis technique. The nanocubes are single crystals with a face-centered-cubic structure. Then, the Ag nanocubes were titrated with an aqueous solution of AuCl_4^- . Au/Ag nanoboxes were formed by the galvanic replacement reaction between Ag and AuCl_4^- . The Au/Ag nanoboxes and Ag nanocubes used as reference samples were mounted on 100-nm-thick SiN membranes.

The coherent X-ray diffraction experiments were carried out at beamline **BL29XUL**. Figure 1 shows a schematic drawing of the apparatus used. The X-ray energy was tuned to 11.8 keV with an undulator gap and a Si (111) double-crystal monochromator. The X-ray beam was two-dimensionally focused to a spot of ~1 μm size by Kirkpatrick-Baez (KB) mirrors. An isolated Ag nanocube or Au/Ag nanobox was placed at the focus in each measurement and illuminated with the focused X-ray beam. Since the nanoparticles are much smaller than the focal spot size, the illuminated X-ray beam is considered to be an X-ray plane wave. The diffracted X-ray photons were detected by an in-vacuum front-illuminated charge-coupled device

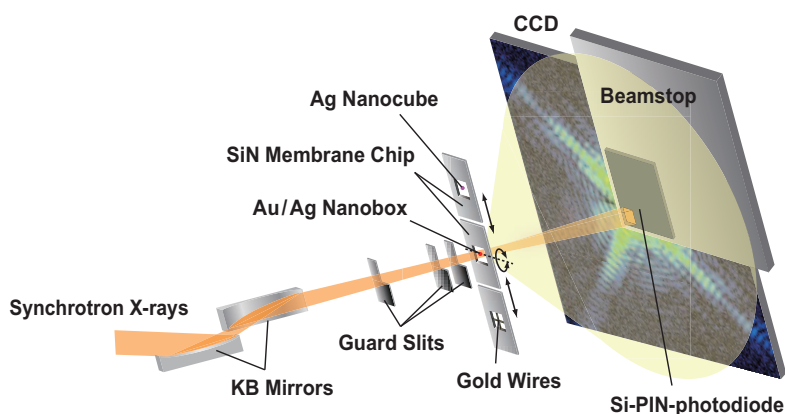


Fig. 1. Schematic view of coherent hard X-ray diffraction measurements of Ag nanocube and Au/Ag nanobox. KB mirrors were placed in air ~100 m downstream of the light source. X-rays with a beam size of 100 μm in both directions illuminated the first mirror. The X-ray beam was 2D focused in a vacuum chamber 445 mm downstream of the second mirror. The focal profile was measured by the wire scanning method using gold wires of 200 μm diameter. To interrupt parasitic scattering X-rays from the mirrors, three guard slits were placed between the mirrors and the focus. An isolated Ag nanocube or Au/Ag nanobox was placed at the focus in each measurement. Forward-diffracted X-ray photons were detected by the CCD detector with a pixel size of 20 \times 20 μm^2 placed 996 mm downstream of the sample. A direct X-ray beamstop was placed in front of the CCD detector. The intensity of the penetrating X-ray beams was monitored using a Si-PIN photodiode, which was assembled on the beamstop, during the measurement of diffraction intensity. The SiN membrane chip, supporting Au/Ag nanoboxes, was rotated for 3D diffraction microscopy.

(CCD) detector. In the data analysis, we used 1251×1251 pixel data, which provided a reconstructed image with a single pixel (or a voxel) size of 4.2 nm in each dimension. Diffraction data were collected at different incident angles ranging from -75° to $+72.5^\circ$ at intervals of 2.5° for the Au/Ag nanobox and of 0° for the Ag nanocube. The X-ray exposure times ranged between 250 s and 1650 s at each incident angle.

The reconstruction of a 3D image was performed by the hybrid input-output method with the Shrinkwrap algorithm. Using the intensities of the reconstructed image of the Ag nanocube used as the reference sample, the flux density at the focus was estimated to be 3.4×10^3 photons/nm²/s. The image intensity of the Au/Ag nanobox is converted to electron units using the flux density. The maximum number of electrons per voxel in the 3D reconstruction was 3.4×10^5 , which was in good agreement with the 3.5×10^5 electrons per $4.2 \times 4.2 \times 4.2$ nm³, corresponding to the voxel size, calculated using the density of the gold crystal with the face-centered-cubic structure, atomic number, and Avogadro's number. Figure 2(a) shows the isosurface rendering of the reconstructed 3D image. The distinctive features of the nanobox are small pits indicated by blue arrows and a depression indicated by a green arrow. The other faces are relatively flat. In previous works, a pinhole was observed on one of the six faces of each cube in the initial stage of reaction, indicating that the reaction was initiated locally at a high-energy site rather than over the entire cube surface. It is possible that the pits on the surface are related to the reaction in the initial stage.

To quantitatively visualize the 3D internal structure, we produced cross-sectional images in the A-, B-, and C-planes parallel to the *xy*-plane. Figure 2(b) shows the cross-sectional images in the A-, B-, and C-planes indicated in Fig. 2(a), which are shown in electron units. The hollow interior is clearly visible in each image. In the B-plane crossing the center of the nanobox, the interior space is larger and the wall is thinner than those in the A- and C-planes. This indicates that the progression rate of the replacement reaction between Ag and HAuCl₄ differs depending on the site. The maximum value of the color bar is 3.4×10^5 electrons. We can roughly identify Au-rich and Au-poor regions in each slice. Areas from yellow to white are Au-rich regions, where more than 50% Ag atoms are replaced with Au atoms. The interesting feature observed is that the Au-rich region exists close to the edges. This suggests that dealloying and morphological reconstruction start from the edges of the nanobox. The spatial resolution of the present 3D diffraction microscope was estimated to be 10 nm or higher from the thinnest wall in the B-plane, which is the highest resolution achieved in 3D hard X-ray

diffraction microscopy. In the near future, ultimate X-ray diffraction microscopy will be realized, which is high-resolution imaging on a short time scale for studying structural dynamics, which will be realized using focused hard X-ray free electron lasers.

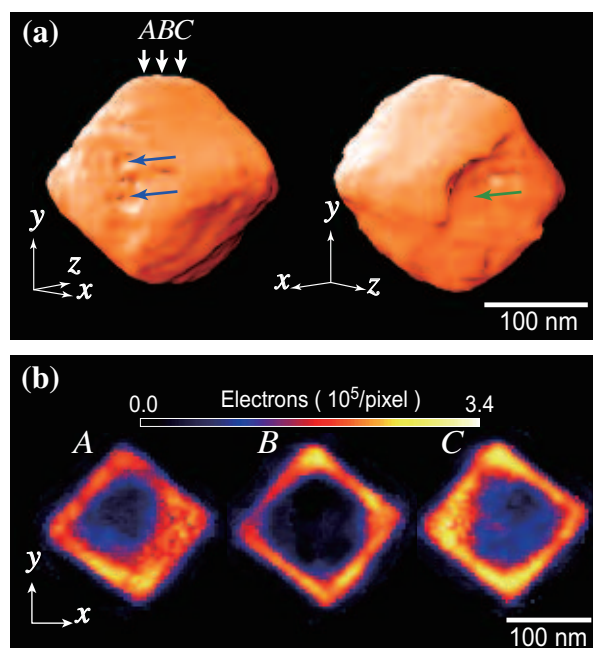


Fig. 2. (a) Isosurface rendering of reconstructed 3D Au/Ag nanobox observed from two directions, which was drawn with a threshold value of 20% of the highest electron density. The small pits and the depression on the surface of the nanobox are clearly visible, which are indicated by blue and green arrows, respectively. (b) Cross-sectional images of a 3D reconstruction of a Au/Ag nanobox. Each image is a cross-sectional image in the A-, B-, and C-planes parallel to the *xy*-planes shown in (a). The distance between two adjacent planes is 33.6 nm. The thickness of each slice is 4.2 nm, corresponding to voxel size.

Yukio Takahashi^{a,*} and Nobuyuki Zettsu^b

^aGraduate School of Engineering, Osaka University

^bGraduate School of Engineering, Nagoya University

*E-mail: takahashi@prec.eng.osaka-u.ac.jp

References

- [1] Y. Xia and N. J. Halas: MRS Bulletin **30** (2005) 338.
- [2] J. Miao *et al.*: Nature **400** (1999) 342.
- [3] Y. Takahashi *et al.*: J. Appl. Phys. **105** (2009) 083106.
- [4] Y. Takahashi *et al.*: Phys. Rev. B **80** (2009) 054103.
- [5] Y. Takahashi *et al.*: Phys. Rev. B **82** (2010) 214102.
- [6] Y. Takahashi, N. Zettsu, Y. Nishino, R. Tsutsumi, E. Matsubara, T. Ishikawa and K. Yamauchi: Nano Letters **10** (2010) 1922.